

# Impacts of Correlated Input Variables

Saliha Arezki\*<sup>‡</sup>, Mohamed Boudour\*

\*Laboratory of Electrical and Industrial Systems, University of Sciences and Technology, Houari Boumediene

sarezki@usthb.dz, mboudour@ieee.org

<sup>‡</sup>Corresponding Author; Saliha Arezki, Laboratory of Electrical and Industrial Systems, University of Sciences and Technology, Houari Boumediene, Bp 32 EL ALIA, Bab Ezzouar- Algiers, ALGERIA, +213 21 20 76 69, sarezki@usthb.dz

Received: 06.07.2012 Accepted: 25.10.2012

**Abstract-** The current trend is moving towards the exploitation of renewable energy especially wind energy. This energy controlled and maximized in power (MPPT) is exploited through system containing a double-fed induction generator (DFIG) driven by the rotor through static converters via the network. For a better quality produced by the wind energy production system, we use multilevel inverters, whose several works lifted problems of fluctuation at the levels of the input voltages. Especially of the five-level neutral point clamping (NPC) voltage source inverter (VSI). This constituted the major limitation for the uses of this power converter. Our contribution lies in the stabilization of the different input voltages of the inverter using a feedback loop control to regulate the average total DC voltage of the inverter by using proportional integrator regulator (PI) and fuzzy logic controller (FLC). To improve the regulation of the input DC voltages, we introduce a power electronic circuit composed of a transistor in series with a resistor. These transistors are controlled to stabilize the input voltages of the inverter. The results obtained show that the use of the five-level NPC VSI in wind system is full of promise on condition to solve the instability problem of the input voltages.

**Keywords-** Wind energy, MPPT, DFIG, five-level NPC, PI regulation, fuzzy logic regulation, clamping bridge.

## 1. Introduction

The use of energy from fuels is the main source of pollution of our planet and we arrive to the exhaustion of its availability. The nature offers free, inexhaustible, available sources of energies in all the regions and respects the environment. These energies are called renewable energies [1].

Among all the renewable energies contributing to the electricity production, the wind energy holds at present the leading part, it is one of the most promising, in terms of ecology, competitiveness, field of application and creation of jobs and wealth. In the scale world, the wind energy since around ten years maintained a growth of 20% per year “Figure 1” [1,2].

Several examples of countries which managed to exploit this energy. The table below gives the top 10 wind power countries where China, United states and Germany holds at present the leading part [1,2].

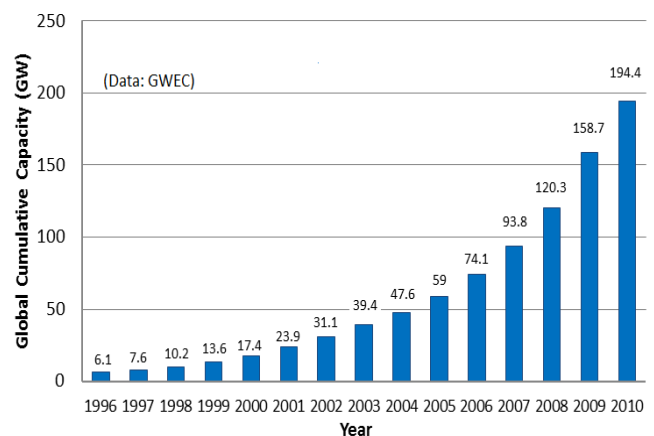
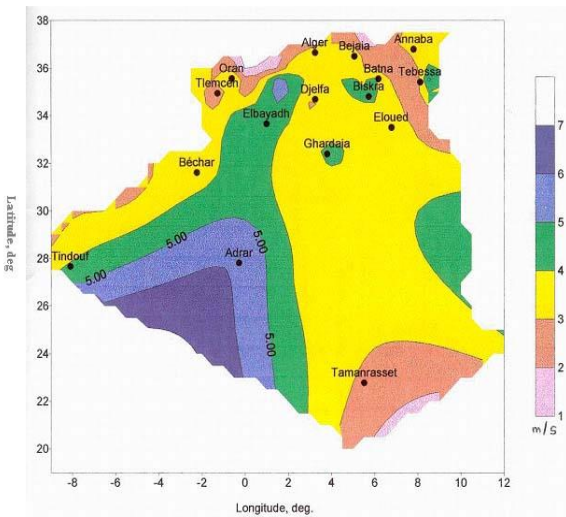


Fig. 1. Global wind power cumulative capacity.

For Algeria, this country practically has no wind plant in spite of the existence of the climatic conditions, seen that the wind reaches intensities around 6 - 7 m/s in the regions of the South-West, “Figure 2”. Moreover, this speed is more than enough to power generation of high power that can be used in the oil zones and for domestic consumption.

**Table 1.** Top 10 wind power countries.

Country	Total capacity end 2009 (MW)	Total capacity June 2010 (MW)	Total capacity end 2010 (MW)	Total capacity June 2011 (MW)
China	26,010	33,800	44,733	52,800
United States	35,159	36,300	40,180	42,432
Germany	25,777	26,400	27,215	27,981
Spain	19,149	19,500	20,676	21,150
India	10,925	12,100	13,066	14,550
Italy	4,850	5,300	5,797	6,200
France	4,521	5,000	5,660	6,060
United Kingdom	4,092	4,600	5,204	5,707
Canada	2,550	3,319	4,008	4,611
Portugal	3,357	3,465	3,734	3,960
Rest of world	21,698	24,500	26,154	29,500
<b>Total</b>	<b>159,213</b>	<b>175,000</b>	<b>196,630</b>	<b>215,000</b>



**Fig. 2.** Preliminary map of the winds in Algeria.

For this reason we chose the study of wind energy. The wind system proposed is based on a double-fed induction generator (DFIG) piloted by the rotor through static

converters (inverter-rectifier). The stator is directly connected to the networks.

To improve the shape of the voltages supplied by the inverter with minimum harmonic distortion, we use multilevel converters. A serious constraint in a multilevel inverter is the capacitor voltage balancing problem [3]. The unbalance of the different DC voltages sources of the five-level NPC VSI constituted the major limitation for the use of this power converter [3-5].

We propose in this paper to study a chain of conversion of energy constituted by a cascade of double fed induction generator driven by a wind system controlled by an enslavement of speed and piloted in the rotor via an inverter and rectifier of five-level NPC structure. The stator is directly connected to the network. The study shows the effect of the stability problem of the DC voltages on the perf DFIG. To remedy to this problem, we propose solutions which use feedback control by a regulation in closed loop control using PI regulation and fuzzy logic regulation. We add clamping bridge to improve the regulation. The results obtained confirm the good performances of the proposed solution.

**2. Presentation of the system studies and problematic**

The production chain studied consists of a double-fed induction generator (7,5kW) [1] driven by a turbine (10kW) [1] through a gearbox or multiplier. The rotor of the machine is excited by the network through static converters. The stator is directly connected to the network. The proposed chain is shown in “Figure 3”.

For a better quality produced by the wind energy chain, we use multilevel converters particular type five-level NPC. Several works [4-7] raised problems of fluctuation at the input voltages of the inverter of five-level NPC structure inducing instability of the voltages supplied.

In this optics we draw our study which lies to resolve the problem of instability of the voltages of the five-level NPC inverter by an enslavement of the input average voltage of the inverter by a fuzzy logic controller.

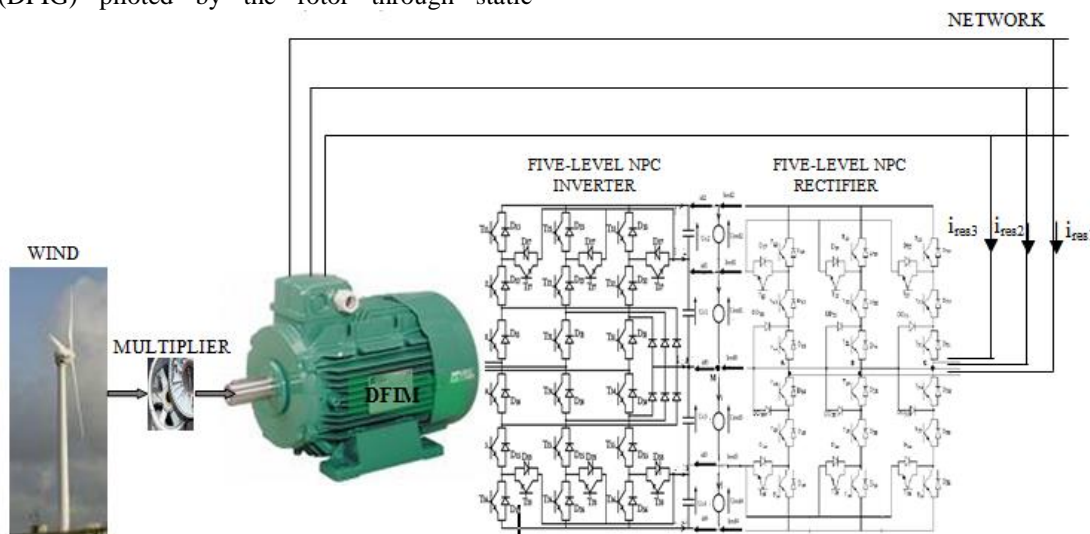


**Fig. 3.** Schematic of the wind system.

**3. Modeling of the Wind Turbine with Maximization of the Power**

*3.1. Modeling of the Wind Turbine*

A wind turbine converses in two parts: a mechanical part (the aeroturbine) and the electric part (the generator) as shown on the ‘‘Figure 4’’ [1,2].

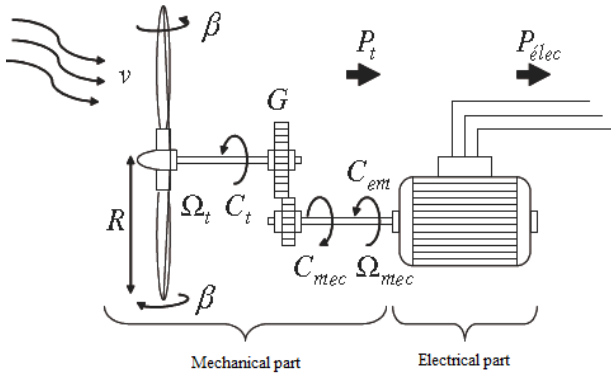


**Fig. 4.** Configuration of a wind turbine

The aeroturbine is constituted by three directional pales of length R basic salaries on one tree of training turning in a speed  $\Omega_{turbine}$ , itself connected with a multiplier of speed of gain G which leads the generator in the speed  $\Omega_{mecanical}$  [1,4,9]. The elasticity and the frictions of pales as well as those of the multiplier will be ignored.

The multiplier is characterized by the gain G adjusts the speed (slow) of the turbine to the generator speed. It is modeled mathematically by the following relations:

$$\Omega_{mecanical} = G \cdot \Omega_{turbine} \tag{1}$$

$$C_g = C_{aer} / G \tag{2}$$

$C_g$  is the mechanical torque of the turbine

$C_{aer}$  is the aerodynamic torque of the turbine is directly determined by:

$$C_{aer} = P_{aer} / \Omega_{turbine} \tag{3}$$

The aerodynamic power recovered at the rotor of the turbine  $P_{aer}$  is:

$$P_{aer} = C_p(\lambda, \beta) (\rho / 2) V^3 S \tag{4}$$

Where:  $\beta$  is The pitch angle

The speed ratio  $\lambda$  is defined as:

$$\lambda = \Omega_{turbine} R / V \tag{5}$$

V is the Wind speed.

The power coefficient  $C_p$ , is the aerodynamic efficiency of the turbine. Its theoretical limit is given by the Betz limit. In our case the power coefficient  $C_p$  is given by the following equation [2]:

$$C_p(\lambda, \beta) = C_1 ((C_2 / \lambda_i) - C_3 \beta - C_4) \exp[-C_5 / \lambda_i] + C_6 \lambda \tag{6}$$

With :  $\lambda_i = (1 / (\lambda + 0.008 \beta) - (0.035 / (\beta^3 + 1)))$

And:  $C_1=0.5176$ ;  $C_2=116$ ;  $C_3=0.4$ ;  $C_4=5$ ;  $C_5=21$ ;  $C_6=0.0068$

The generator shaft is modeled by the following equation:

$$J d\Omega_{mecanical} / dt = C_g - C_{em} - f \Omega_{mecanical} \tag{7}$$

J is the total inertia of rotating parts ( $Kg \cdot m^2$ ).

f is the viscous friction coefficient.

$C_{em}$  the electromagnetic torque of the generator (N.m).

By neglecting the losses of origin electric, the electric power becomes equal to the electric power defined by:

$$P_{elec} = C_{em} \cdot \Omega_{mecanical} \tag{8}$$

*3.2. Maximization of the Power with Speed Control*

The wind turbines used for power generation must be able to produce maximum power by making the most of available energy in the wind. This is called search of the functioning point at maximum power (MPPT) [2]. The use of a wind turbine with variable speed allows maximizing this power. It is thus necessary to conceive strategies of command allowing to maximize the electric generated power (thus the torque) by adjusting the rotational speed of the turbine at its reference value [2].

The block diagram of maximizing the power extracted with speed control is represented by the ‘‘Figure 5’’ [2]. The corrector considered for the enslavement of the speed is the regulator proportional-integral (PI).

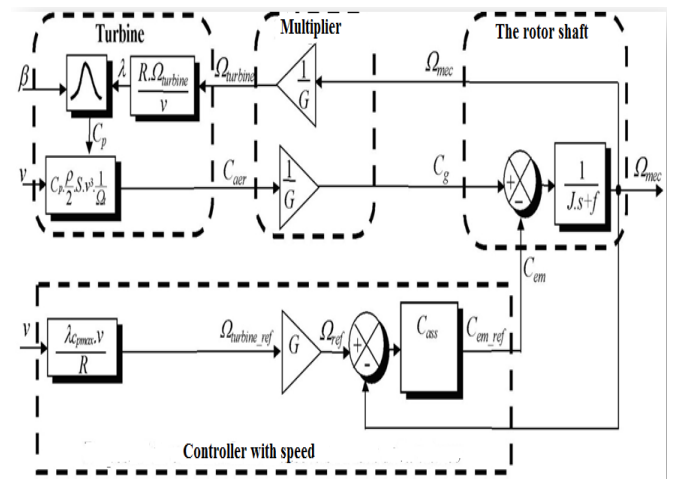


**Fig. 5.** MPPT with speed enslavement

The wind profile used in our model is shown in ‘‘Figure 6’’ and the variation of the mechanical speed of the generator, which turns at 157rad / s, or around 1500rpm and follows its reference.

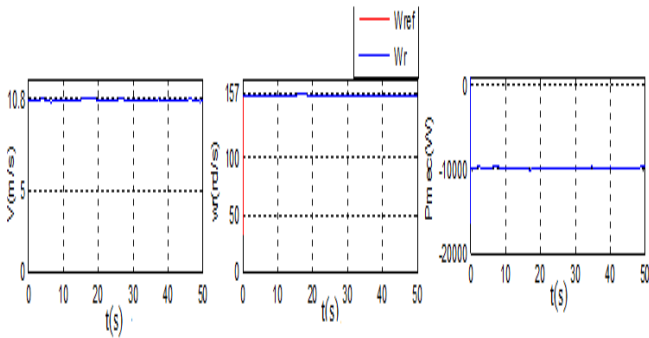


**Fig. 6.** Wind profile model applied and the mechanical speed of the generator and mechanical output

**4. Modeling of the DFIG with Regulation of Power in Closed Loop**

*4.1. Modeling of the Generator*

The generator chosen for the conversion of kinetic energy is the double-fed induction generator (DFIG). We opt for a DFIG driven by the rotor, this choice allows for a single converter designed for a nominal power of about 25% to 30% of the nominal power [1,2,9]. Thus, it will be less voluminous, less expensive and will require a less cumbersome cooling system [1,2,9]. The modeling of the DFIG in frame of PARK is given as follow [4,9]:

$$\begin{cases} V_{ds} = R_s i_{ds} + \frac{d}{dt} \Phi_{ds} - \omega_s \Phi_{qs} \\ V_{qs} = R_s i_{qs} + \frac{d}{dt} \Phi_{qs} + \omega_s \Phi_{ds} \end{cases}$$

$$\begin{cases} V_{dr} = R_r i_{dr} + \frac{d}{dt} \Phi_{dr} - (\omega_s - \omega) \Phi_{qr} \\ V_{qr} = R_r i_{qr} + \frac{d}{dt} \Phi_{qr} + (\omega_s - \omega) \Phi_{dr} \end{cases} \quad (9)$$

$$Cem = p \frac{M}{L_s} (\Phi_{qs} i_{dr} - \Phi_{ds} i_{qr})$$

*4.2. Control power of the double fed induction generator*

In order to easily control the production of electricity by the wind turbine, we will carry out an independent control of active and reactive powers by orientation of the stator flux.

By choosing a reference frame linked to the stator flux, rotor currents will be related directly to the stator active and reactive power. An adapted control of these currents will thus permit to control the power exchanged between the stator and the grid. If the stator flux is linked to the d-axis of the frame we have [9]:

$$\Phi_{ds} = \Phi_s ; \Phi_{qs} = 0 \quad (10)$$

In any diphas reference, the active and reactive statoric powers of an induction machine are written [9]:

$$\begin{cases} P = V_{ds} i_{ds} + V_{qs} i_{qs} \\ Q = V_{qs} i_{ds} - V_{ds} i_{qs} \end{cases} \quad (11)$$

Assuming the flux is kept constant  $\Phi_{ds}$  (which is ensured by the presence of a stable network connected to the stator); the choice of this reference makes the electromagnetic couple produced by the machine, and consequently the active power, only dependent on the rotoric current of axis q. Moreover if we neglect the resistance of the winding statoric  $R_s$ , which is a rather realistic hypothesis for the machines of strong power used for the wind production, the adaptation of the equation (11) to the simplifying hypotheses gives [1,9]:

$$\begin{cases} P_{ref} = -V_s \frac{M}{L_s} i_{qr} \\ Q_{ref} = \frac{V_s \Phi_s}{L_s} - \frac{V_s M}{L_s} i_{dr} \end{cases} \quad (12)$$

Considering these powers as the reference, the set of reactive power is kept zero in order to keep a unity power factor rated stator [1,9].

The diphas components of rotor voltages to be imposed on the machine to obtain the desired rotor currents are:

$$\begin{cases} V_{dr} = R_r i_{dr} + (L_r - \frac{M^2}{L_s}) \frac{d}{dt} i_{dr} - g \omega_s (L_r - \frac{M^2}{L_s}) i_{qr} \\ V_{qr} = R_r i_{qr} + (L_r - \frac{M^2}{L_s}) \frac{d}{dt} i_{qr} - g \omega_s (L_r - \frac{M^2}{L_s}) i_{dr} + g \frac{M V_s}{L_s} \end{cases} \quad (13)$$

From these equations, we can establish the relation between the voltages applied to the rotor of the machine and the statoric powers that it engenders. It is thus possible now to describe the block scheme which is composed of two loops, an inner current loop and an outer power loop. Control systems are shown in ‘Figure 7’ [1].

The aim of Proportional Integral controller (PI) used is to obtain high dynamic performances in terms of reference tracking and sensitivity to perturbations.

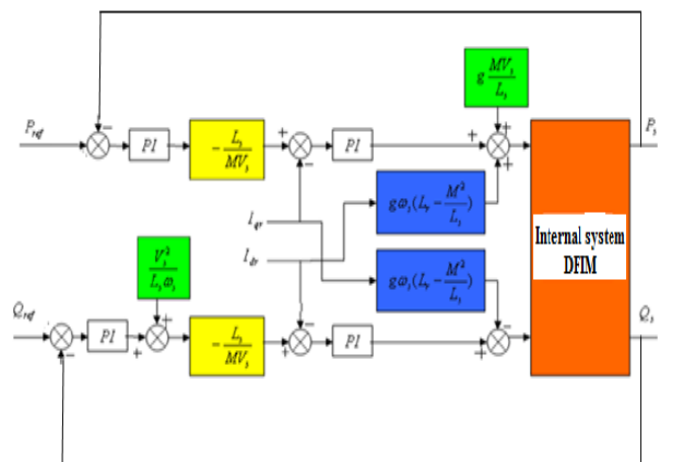


**Fig. 7.** Block scheme of the structure of indirect control by stator flux

**5. Modeling and Control of Five-level NPV VSI**

*5.1. Structure of five-level NPC VSI*

The five-level NPC VSI is one of the structure of power conversion used to feed great power AC loads. The “Figure 8” presents the structure of the three phase’s five-level NPC voltage source inverter [4,5,6]. This inverter is constituted by three arms and four DC voltages sources. Every arms has eight bi-directional switches; six in series and two in parallel and two diodes DDi0 and DDi1 which let have zero voltage for VKM (VKM is the voltage of the phase K relatively to the middle point M) [4-6]. Several complementary laws are possible for five-level NPC VSI [7,8,10]. The optimal complementary law used for this converter is presented below [4-6]:

$$B_{i4} = \bar{B}_{i2} \quad , \quad B_{i5} = \bar{B}_{i1} \quad , \quad B_{i6} = \bar{B}_{i3} \tag{14}$$

$B_{is}$  : Control signal of the semiconductor  $TD_{is}$ ,

In a controllable mode, we define for each semiconductor  $TD_{is}$ , using the proposed complementary law, a connection function  $F_{is}$  as follow [4-6,8,9]:

$$F_{is} = \begin{cases} 1 & \text{if } TD_{is} \text{ is closed} \\ 0 & \text{if } TD_{is} \text{ is opened} \end{cases} \tag{15}$$

The input voltage of the inverter, relatively to the middle point M, is given by the following system [4,5,6]:

$$\begin{aligned} V_{KM} = & F_{i1}F_{i2}(1 - F_{i3})U_{C1} + F_{i1}F_{i2}F_{i3}(U_{C1} + U_{C2}) - \\ & F_{i4}F_{i5}(1 - F_{i6})U_{C3} - F_{i4}F_{i5}F_{i6}(U_{C3} + U_{C4}) \end{aligned} \tag{16}$$

Where  $K \in \{A, B, C\}$  and respectively  $i \in \{1, 2, 3\}$

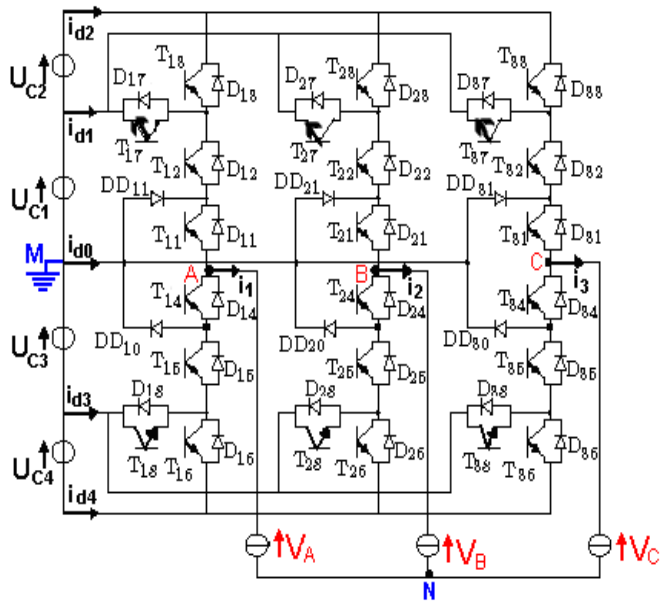
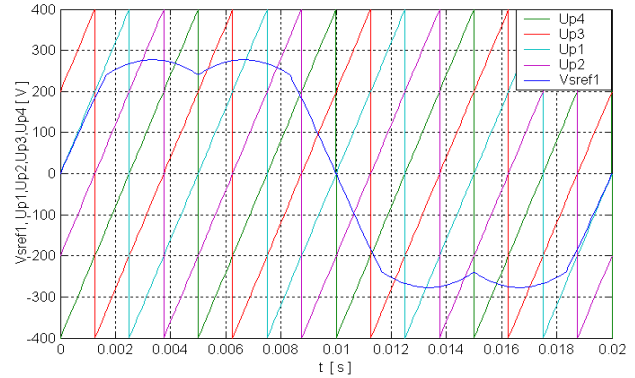


**Fig. 8.** Three-phase five-level NPC configuration

*5.2. PWM Strategy of the five-level NPC VSI*

Different PWM algorithms of the five-level NPC VSI are possible, one of them is the vector modulation strategy with four bipolar carriers [4-6], and the “Figure 9” shows his signal. This strategy is characterized by modulation index (m) and modulation rate (r) [4-6].



The principle of this strategy as its name suggests, allows users to follow the vector voltage reference. It sets from vector reference  $V_{sref}$ ,  $V_{sref} = (V_{ref1}, V_{ref2}, V_{ref3})t$  vector of a new reference  $V_{sref1}$  associated with half-arm at the top and bottom define as follows [4-6]:

$$V_{sref1}[i] = V_{sref}[i] + V_0 \quad (i=1,2,3) \tag{17}$$

The voltage  $V_0$  Frequency  $3f$ , is given by the following expression:

$$V_0 = - \frac{[\max(V_{sref}) + \min(V_{sref})]}{2} \tag{18}$$

**6. Modeling and Control of Five-Level PWM Current Rectifier**

*6.1. Modeling of the Five-Level PWM Rectifier*

The reversibility of the five-level NPC VSI allows it to work as current rectifier, “Figure 10”[3].

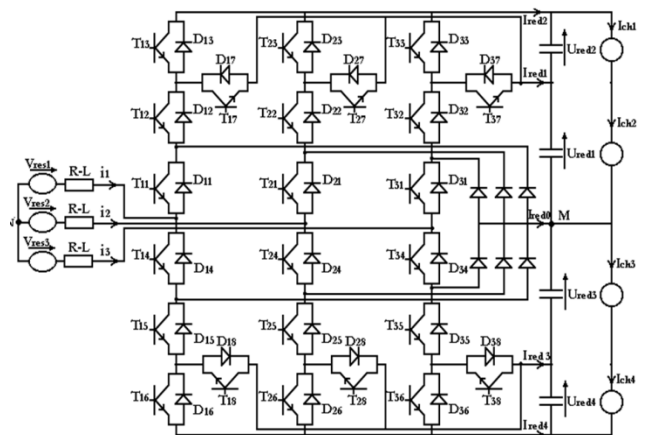


**Fig. 10.** Structure of the five-level PWM current rectifier

The input voltages of the five-level PWM rectifier are defined as follows:

$$\begin{bmatrix} V_A \\ V_B \\ V_C \end{bmatrix} = \frac{1}{3} \begin{bmatrix} 2 & -1 & -1 \\ -1 & 2 & -1 \\ -1 & -1 & 2 \end{bmatrix} \left\{ \begin{array}{l} \begin{bmatrix} F_{17} + F_{11}^b \\ F_{27} + F_{21}^b \\ F_{37} + F_{31}^b \end{bmatrix} U_{red1} - \begin{bmatrix} F_{11}^b \\ F_{21}^b \\ F_{31}^b \end{bmatrix} U_{red2} \\ - \begin{bmatrix} F_{28} + F_{10}^b \\ F_{28} + F_{20}^b \\ F_{28} + F_{30}^b \end{bmatrix} U_{red3} - \begin{bmatrix} F_{10}^b \\ F_{20}^b \\ F_{30}^b \end{bmatrix} U_{red4} \end{array} \right\} \quad (19)$$

The rectifier output currents are:

$$\begin{cases} i_{red1} = F_{17} i_{res1} + F_{27} i_{res2} + F_{37} i_{res3} \\ i_{red2} = F_{11}^b i_{res1} + F_{21}^b i_{res2} + F_{31}^b i_{res3} \\ i_{red3} = F_{18} i_{res1} + F_{28} i_{res2} + F_{38} i_{res3} \\ i_{red4} = F_{10}^b i_{res1} + F_{20}^b i_{res2} + F_{30}^b i_{res3} \end{cases}$$

$$\begin{aligned} i_{red0} &= (i_{res1} + i_{res2} + i_{res3}) - (F_{17} + F_{18} + F_{11}^b + F_{10}^b) i_{res1} \\ &\quad - (F_{27} + F_{28} + F_{21}^b + F_{20}^b) i_{res2} \\ &\quad - (F_{37} + F_{38} + F_{31}^b + F_{30}^b) i_{res3} \end{aligned} \quad (20)$$

6.2. Hysteresis-Band Current Control

All possible control strategies for five-level inverter are used for five-level PWM rectifier [4]. In this paper, we choose the current hysteresis strategy to control this rectifier to obtain network weak current harmonics rate and power factor part near unity. Its strategy algorithm is given as follow:

$$\begin{cases} \text{Si } \varepsilon_k > 2\Delta i \Rightarrow B_{k1} = 0; B_{k2} = 0; B_{k3} = 0 \\ \text{Si } \Delta i < \varepsilon_k < 2\Delta i \Rightarrow B_{k1} = 0; B_{k2} = 0; B_{k3} = 1 \\ \text{Si } -\Delta i < \varepsilon_k < \Delta i \Rightarrow B_{k1} = 1; B_{k2} = 0; B_{k3} = 0 \\ \text{Si } -2\Delta i < \varepsilon_k < -\Delta i \Rightarrow B_{k1} = 1; B_{k2} = 1; B_{k3} = 0 \\ \text{Si } \varepsilon_k < -2\Delta i \Rightarrow B_{k1} = 1; B_{k2} = 1; B_{k3} = 1 \end{cases} \quad (21)$$

$$\xi_k = i_{resk} - i_{refk} \quad (k=1,2,3)$$

$\Delta_i$ : Hysteresis band width

7. Modeling of the DC Bus Voltages

The ‘Figure 11’ shows the structure of the DC bus [5,7,8,10].

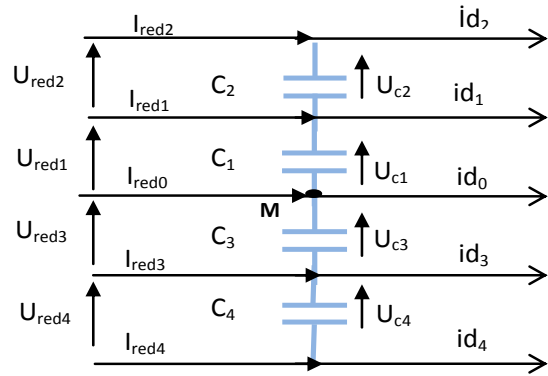


Fig. 11. Structure of the DC voltages bus.

The model of this DC bus is defined as follow [5,7,8,10]:

$$\begin{cases} C_1 \frac{dU_{c1}}{dt} = i_{red1} + i_{red2} - i_{d1} - i_{d2} \\ C_2 \frac{dU_{c2}}{dt} = i_{red2} - i_{d2} \\ C_3 \frac{dU_{c3}}{dt} = i_{d3} + i_{d4} - i_{red4} - i_{red3} \\ C_4 \frac{dU_{c4}}{dt} = i_{d4} - i_{red4} \end{cases} \quad (22)$$

8. Simulation Results and Comments

The results of simulation of the complete chain of wind conversion are shown by the following figures.

Those simulations ‘Figure 12’ show perfectly the problem of the unbalance of the four voltages of the DC bus.

We can see ‘Figure 12’ that the voltages are increasing. The characteristics of the drive of the DFIG ‘Figure 13’ show important undulations of the current, torque which is causing by the instability of the voltage Va.

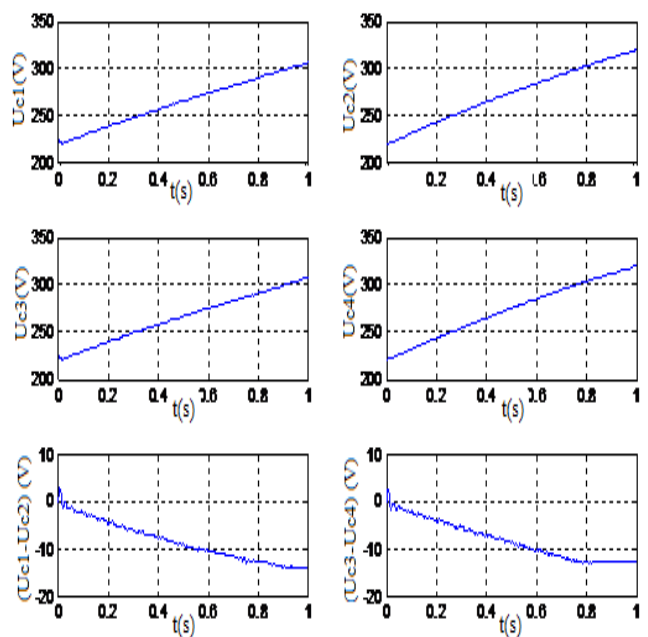


Fig. 12. The DC bus voltages and their differences.

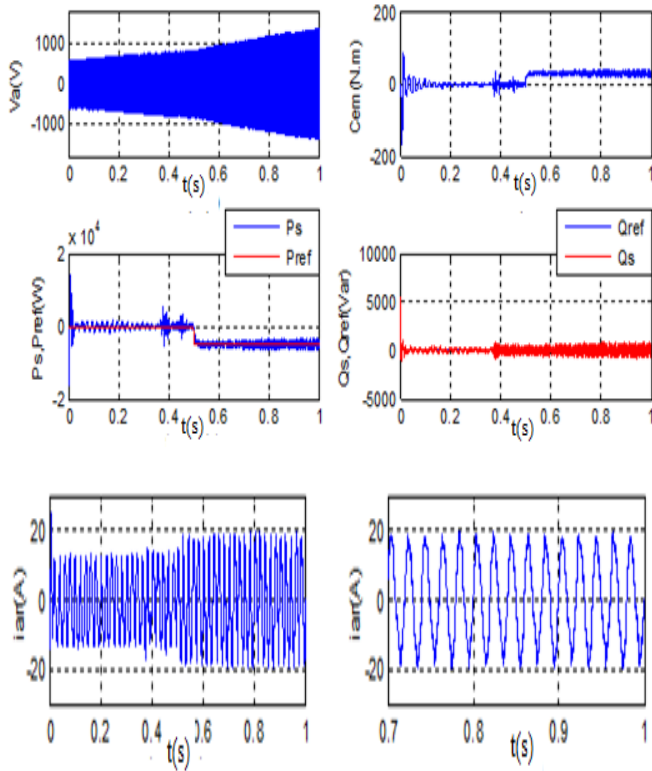


Fig. 13. Performances of DFIG.

To remedy to the problem of the instability of the output DC voltages of PWM rectifier which are also the input voltages of the inverter, we propose feedback control for the voltage loop.

**9. Feedback Control of Five-Level PWM current rectifier**

In this section, we have chosen to compare the variation of the voltages of the DC bus with two different controllers. The proportional- integral will be first tested and will be the reference compared to the fuzzy logic controller.

**9.1. PI Controller**

This controller is simple to elaborate. “Figure 14” shows the block diagram of the system implemented with this controller. The terms *kp* and *ki* represent respectively the proportional and integral gains.

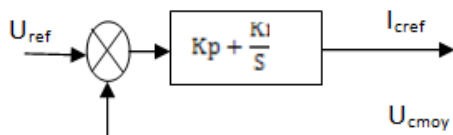


Fig. 14. Integral-proportional regulator structure.

$$U_{ct} = \frac{U_{c1} + U_{c2} + U_{c3} + U_{c4}}{4}$$

The voltage loop “Figure 15” imposes the effective value of the reference current of the network corresponding

to the power exchanged between the network and the continue load.

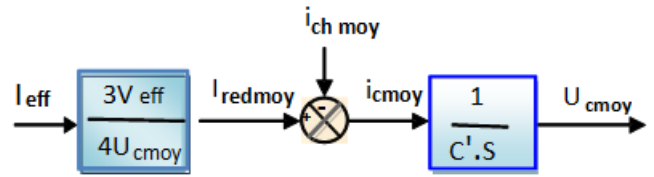


Fig. 15. Five-level rectifier voltage model.

We defined the next value as follows:

$$i_{c_{moy}} = \frac{i_{c1} + i_{c2} + i_{c3} + i_{c4}}{4} ; i_{ch_{moy}} = \frac{i_{ch1} + i_{ch2} + i_{ch3} + i_{ch4}}{4}$$

$$U_{c_{moy}} = \frac{U_{c1} + U_{c2} + U_{c3} + U_{c4}}{4} ; i_{red_{moy}} = (i_{ch_{moy}} + i_{c_{moy}})$$

The general principle enslavement of five-level rectifier is given by “Figure 16”.

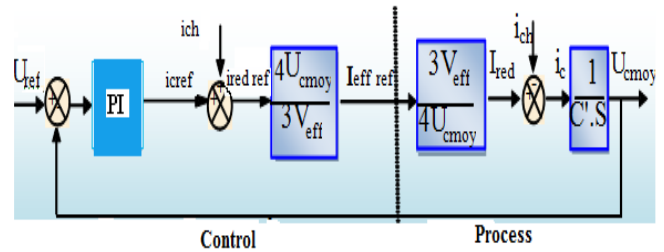


Fig. 16. Enslavement algorithm of output voltage of five-level rectifier.

This regulator presents several disadvantages:

- A zero is present in the numerator of the transfer-function,
- The integrator introduces a phase difference which can induce instability,
- The regulator is directly calculated with the parameters of the filter, if these parameters are varying, the robustness of the system can be affected.

**9.2. Fuzzy Logic Controller**

The control system is based on fuzzy logic. This type of control, approaching the human reasoning that makes use of the tolerance, uncertainty, imprecision and fuzziness in the decision-making process, manages to offer a very satisfactory performance, without the need of a detailed mathematical model of the system just by incorporating the experts’ knowledge into fuzzy rules.

As illustrated in “Figure 17”; this fuzzy logic control is based on mamdani’s system. This system has four main parts. First, using input membership functions, inputs are fuzzified then based on rule bases and inference system, outputs are produced and finally the fuzzy outputs are defuzzified and applied to the main control system. Error of inputs from their references and error deviations in any time interval are chosen as inputs.

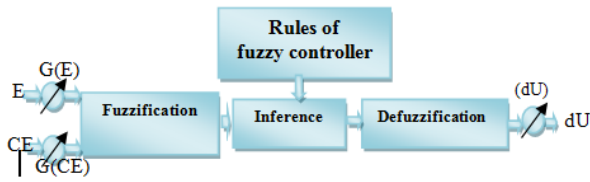


Fig. 17. Basic structure of fuzzy controller.

$$\begin{cases} E = U_{ref} - U_{cmoy} \\ CE = E(k) - E(k-1) \end{cases} \quad (24)$$

The scale factor  $G(E)$ ,  $G(CE)$ ,  $G(dU)$  are changing with the values of inputs and output controller.

The general principle enslavement of five-level rectifier is the same as given in ‘Figure 15’.

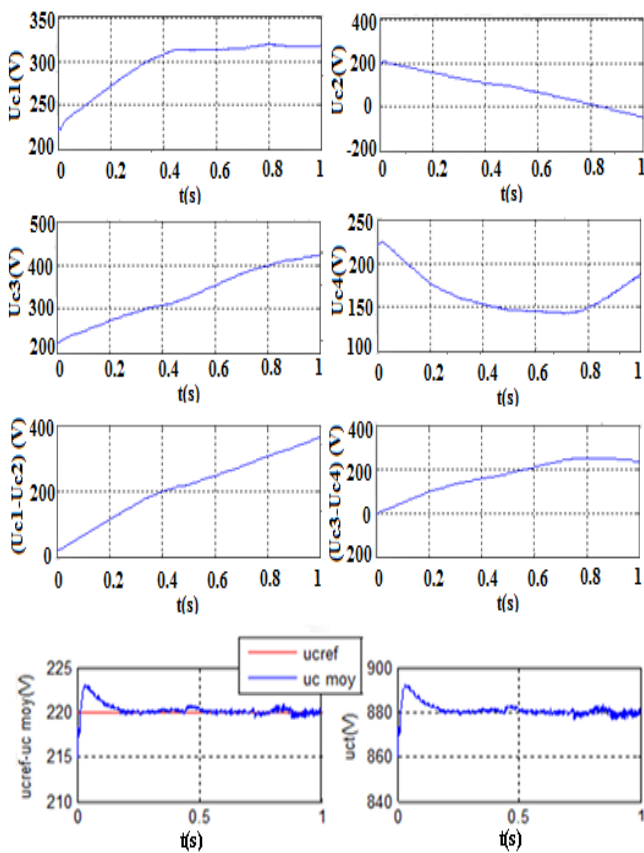


Fig. 18. Output voltages of DC bus voltage.

The ‘Figure 18 and Figure 19’ show the different voltages obtained by the application of the enslavement with two controllers. We remark that the output average voltage of the rectifier is practically stable nevertheless the different input voltages  $U_{ci}$  of the inverter are not. The error of variation of the DC bus voltages with fuzzy logic is lower than the error variation with PI.

For better stabilization of the DC bus voltage, we introduce into the system a chopper based on transistor.

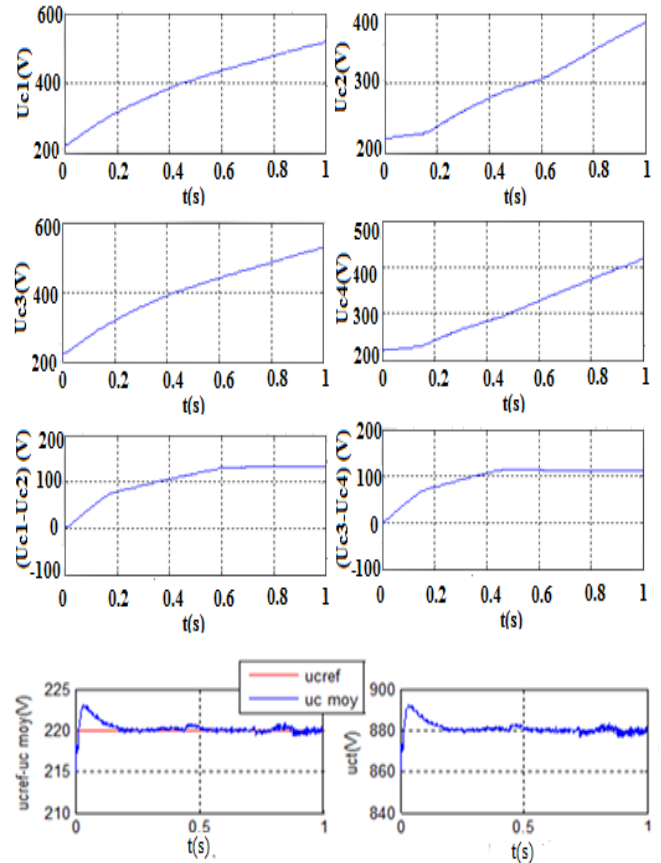


Fig. 19. Output voltages of DC bus voltage and the output voltage of rectifier and his reference.

### 10. Regulation of the Input Voltages of the Inverter by the Power Electronics

This component of power electronics is called clamping bridge. The bridge is a simple circuit consisting of a transistor and a resistor placed in series across each capacity, ‘Figure 20’.

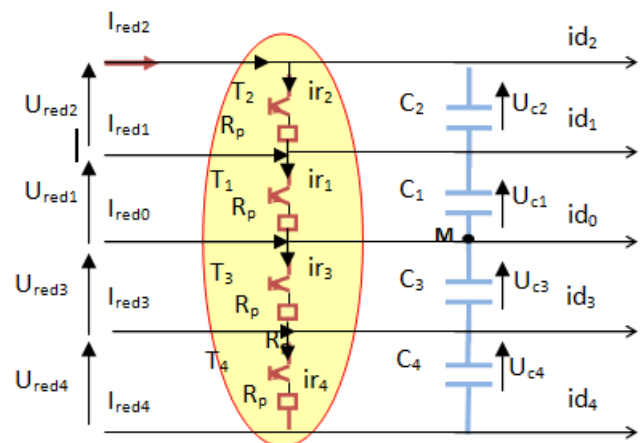


Fig. 20. Structure of the capacitif filter with clamping bridge.

The mathematical model of the intermediate filter with clamping bridge is defined as follows:

$$\begin{cases} C_1 \frac{dU_{c1}}{dt} = i_{red1} + i_{red2} - i_{d1} - i_{d2} - i_{r1} \\ C_2 \frac{dU_{c2}}{dt} = i_{red2} - i_{d2} - i_{r2} \\ C_3 \frac{dU_{c3}}{dt} = i_{d3} + i_{d4} - i_{red4} - i_{red3} - i_{r3} \\ C_4 \frac{dU_{c4}}{dt} = i_{d4} - i_{red4} - i_{r4} \end{cases} \quad (25)$$

These transistors are controlled [8-10] to stabilize the input voltage of inverter. The control algorithm of the clamping bridge is given by [8-10]:

$$i_{ri} = \frac{U_{ci}}{R_p} T_i \text{ if } U_{ci} \geq 200 \text{ else } 0 \quad (i=1 \div 4) \quad (26)$$

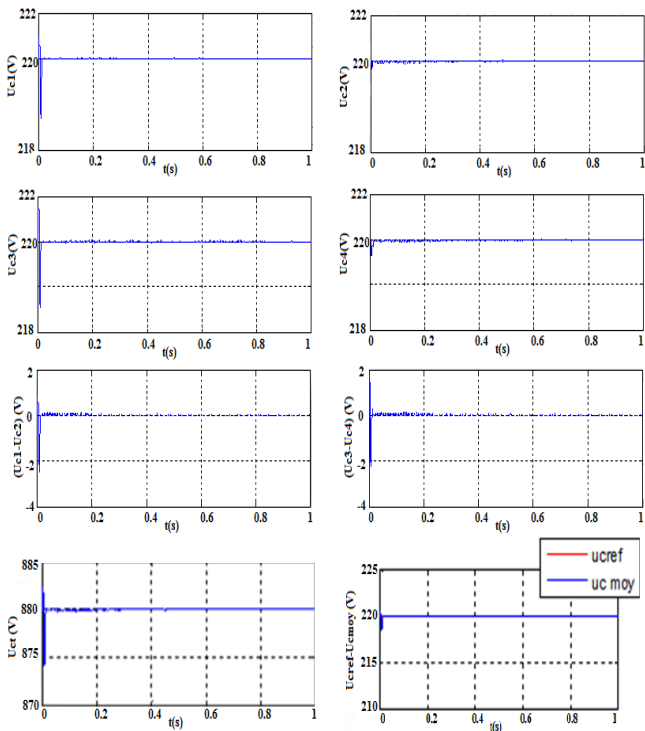


**Fig. 21.** Output voltages of DC bus voltage and the output voltage of rectifier and his reference.

By using the clamping bridge as technique of stabilization, we remark that the input voltages of the five-level NPC VSI stabilize around 220V ‘‘Figure 21’’ and that the undulations on the performances (voltage and current) disappear ‘‘Figure 22’’. ‘‘Figure 23’’ show that the network current follows its reference and the voltage network voltage and current are in phases then the power factor of network is uniting.

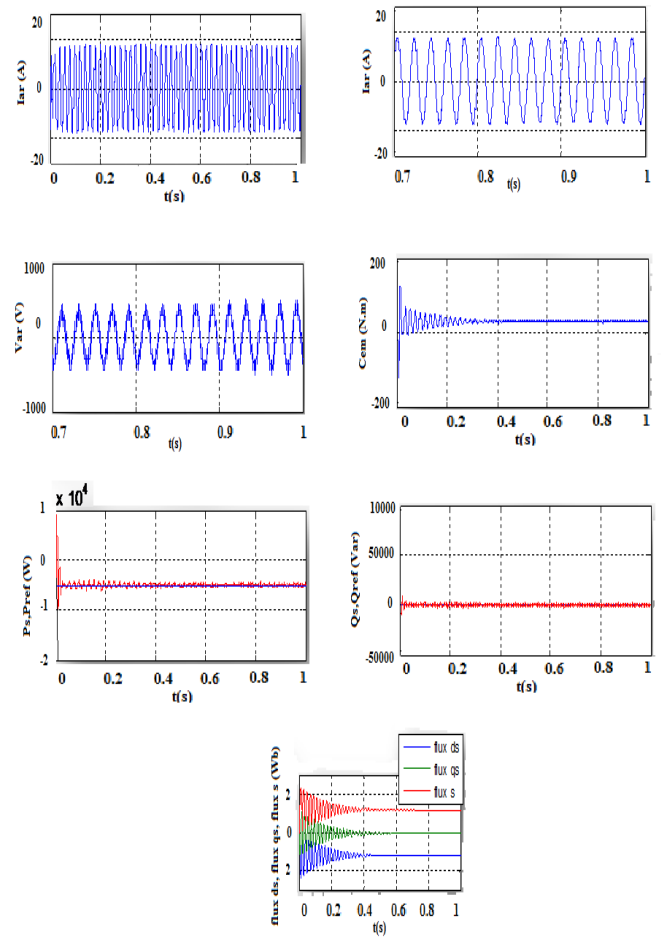


**Fig. 22.** Performances of the DFIG.

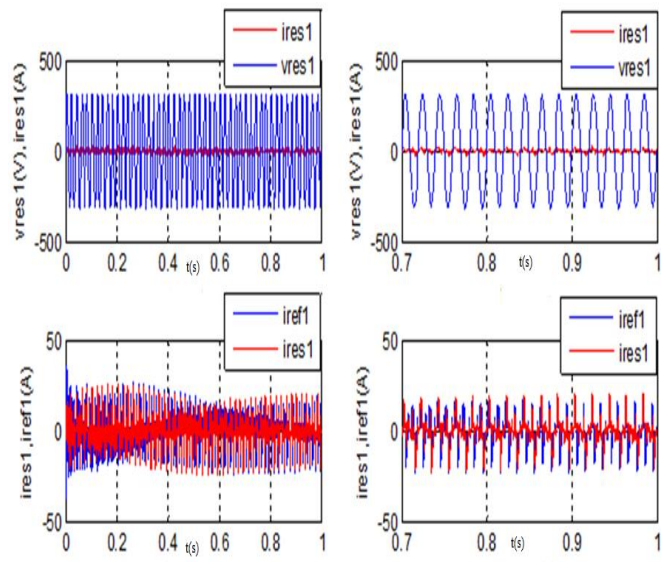


**Fig. 23.** The voltage network, the network current and his reference.

## 11. Conclusion

The major limitation of the use of multilevel inverters is the capacitor voltage balancing problem. In this paper, we have studied stability problem of the input voltages of the five-level NPC VSI by given several solutions for the solving. The application of linear feedback using classical regulator (PI) and fuzzy logic regulator (FL) show perfect following of the total average input voltage of the inverter to its reference but the different input voltages are not perfectly stable with differences no null. Noted that, the regulation by fuzzy logic is more interesting view of point of ripple and stability in steady state. To equalize the DC capacitors voltages in all the levels, we propose to add clamping bridge circuit. Those solutions show the good performances of the wind system.

## Appendix

$V_{eff} = 220V$ ,  $f=50$  Hz,  $f_p=2kHz$ ,  $p_{ref}=-5000W$ ,  $Q_{ref}=0Var$ ,  
 $C_r = -49Nm$ ,  $C_1 = C_2 = C_3 = C_4 = 20mF$ ,  $U_{ref} = U_{cref} = 220V$ ,  
 $\Delta_i = 0.01$ .

## References

- [1] F. Poitiers, "Etude et commande de génératrices asynchrones pour l'utilisation de l'énergie éolienne, machine asynchrone à cage autonome, machine asynchrone à double alimentation reliée au réseau", Université de Nantes, 2003.
- [2] El Aimani, "Modélisation de différentes technologies d'éoliennes intégrées dans un réseau de moyenne tension", Ecole Centrale de Lille, Université des Sciences et Technologies de Lille, 2004.
- [3] R. Chibani and E.M. Berkouk, "Five-level PWM current rectifier- Five-level NPV VSI- Permanent magnet synchronous machine cascade", The European Physical Journal. Applied Physics. 30, 135-148 (2005.)
- [4] S. Arezki, M. Boudour, "Behavior of a Double-fed Asynchronous Machine Supplied by Source: Wind - photovoltaic", International Symposium on Environment Friendly Energies in Electrical Application (EFEEA), 2-4 November 2010, Ghardaïa, Algeria.
- [5] S. Arezki and E.M. Berkouk, "High Voltage of two Batteries-two five-level NPC voltage sources inverters Cascade. Application to the DSIM drive", International Conference on Renewable Energy and Power Quality, ICREPQ'08, Santander, Spain.
- [6] S. Arezki, M. Boudour, F. Bouchafaa, and E.M. Berkouk, "Study of the Stability Voltage of a Frequency Changer using Inverter of Five-Level NPC Structure", 3rd International Conference on Electrical Engineering, Alger, Mai 2009.
- [7] S. Arezki, M. Boudour et E.M. Berkouk., "Conceiver of Cascade AC/AC of Output Bridge Multilevel Inverter. Applied to the DSIM", 3rd International Conference on Electrical Engineering Design and Technologies (ICEEDT'09), Tunisie, Sousse, Octobre 2009.
- [8] S. Arezki, M. Boudour., "Simulation and Modeling of a Photovoltaic System Adapted by a MPPT control reaction: Application on a DSIM", IEEE International Conference & Exhibition, Energycon, December 20-22, 2010, Manama, Bahrain.
- [9] S. Arezki, M. Boudour., "Contribution to the improvement of the performances of a chain of conversion of energy fed by a double source", 2nd International Conference on Advances in Energy Engineering (ICAEE 2011), en December 27-28, 2011, Bangkok, Thailand.
- [10] S. Arezki, M. Boudour., "Simulation of the electric functioning of a photovoltaic system commanded by the method INC and INC improved. Application to the Double star induction machine", 12th International conference on Sciences and Techniques of Automatic control and computer engineering- STA'2011, December 18-19-20, 2011, Sousse, Tunisia.